

## Article

# Production of Therapeutically Significant Genistein and Daidzein Compounds from Soybean Glycosides Using Magnetic Nanocatalyst: A Novel Approach

Mamata Singhvi, Minseong Kim  and Beom-Soo Kim \* 

Department of Chemical Engineering, Chungbuk National University, Cheongju 28644, Korea

\* Correspondence: bskim@chungbuk.ac.kr; Tel.: +82-43-261-2372; Fax: +82-43-269-2370

**Highlights:**

- Production of therapeutical aglycone compounds was attempted using a nanocatalyst.
- The maximum amount of daidzein (8.91 g/L) and genistein (12.0 g/L) was generated at 80 °C in 3 h with yields of 0.590 and 0.621 g/g substrate, respectively.
- Reused nanocatalyst demonstrated ~35% catalytic efficiency even after third recycle.
- Nanocatalyst can be a better substitute for costly enzymes in aglycone production.

**Abstract:** Genistein and daidzein are well-known biologically active pharmaceutical compounds that play significant roles in the treatment of various diseases such as cardiovascular problems, cancer, etc. In some plants, the glycosides daidzin and genistin are present in ample amounts that can be converted into aglycones, daidzein and genistein, through hydrolysis. Here, magnetic cobalt ferrite alkyl sulfonic acid (CoFe<sub>2</sub>O<sub>4</sub>-Si-ASA) nanocatalyst was used for the hydrolysis of glycosides into aglycones. The application of CoFe<sub>2</sub>O<sub>4</sub>-Si-ASA nanocatalyst generated a maximum 8.91 g/L daidzein and 12.0 g/L genistein from 15.1 g/L daidzin and 19.3 g/L genistin with conversion efficiencies of 59.0% and 62.2%, respectively, from soybean glycosides at 80 °C in 3 h. The use of a modern nanocatalyst is preferred over enzymes because of its lower production cost, higher rate of reaction, higher stability, etc. To our knowledge, this is the first report on using nanocatalyst for the production of genistein and daidzein in a sustainable manner.

**Keywords:** cobalt ferrite alkyl sulfonic acid nanocatalyst; soybean; genistin; daidzin; genistein; daidzein;  $\beta$ -glucosidase



**Citation:** Singhvi, M.; Kim, M.; Kim, B.-S. Production of Therapeutically Significant Genistein and Daidzein Compounds from Soybean Glycosides Using Magnetic Nanocatalyst: A Novel Approach. *Catalysts* **2022**, *12*, 1107. <https://doi.org/10.3390/catal12101107>

Academic Editor: Anwar Sunna

Received: 19 July 2022

Accepted: 23 September 2022

Published: 25 September 2022

**Publisher's Note:** MDPI stays neutral with regard to jurisdictional claims in published maps and institutional affiliations.



**Copyright:** © 2022 by the authors. Licensee MDPI, Basel, Switzerland. This article is an open access article distributed under the terms and conditions of the Creative Commons Attribution (CC BY) license (<https://creativecommons.org/licenses/by/4.0/>).

## 1. Introduction

Phytoestrogens are plant-derived compounds possessing health-promoting properties, which are classified into groups such as isoflavones, phytosterols, and lignans [1]. Isoflavones belong to the flavonoid class, which has drawn considerable attention in the medical field chiefly because of their antioxidant and estrogenic activities [2]. Most of the reported studies have designated that particularly the unconjugated forms of isoflavones, i.e., aglycones, exhibit greater beneficial effects than the isolated forms [3]. In general, legumes are the most essential source of isoflavones. Among them, soybean (*Glycine max*) is considered the ultimate source, which principally occurs in the form of  $\beta$ -glucosides [4]. These glycosides can be further hydrolyzed to be converted into their bioactive forms, i.e., aglycone forms, which have a substantial effect on human health [5].

Daidzein (7-hydroxy-3-(4-hydroxyphenyl)-4-benzopyrone) and genistein (5,7-dihydroxy-3-(4-hydroxyphenyl)-4H-1-benzopyran-4-one) are significant isoflavones that are usually present in their respective glycoside forms, daidzin and genistin, in legumes [6]. These aglycone compounds (daidzein and genistein) possess a 7-hydroxyisoflavone frame, which is structurally equivalent to the utmost effective estrogen hormone, estradiol-17 $\beta$ . Owing to the structural

homologies between estrogen and isoflavone compounds, aglycone compounds are capable of binding to estrogen receptors (such as ER $\alpha$  and ER $\beta$ ), which can mimic the estrogenic actions of the antagonistic or agonistic types [7]. Aglycone compounds have been widely used in the treatment of various hormone-associated diseases such as breast cancer, menopausal problems, cardiovascular diseases, osteoporosis, anticarcinogenic, antioxidant, anti-inflammatory, and antimicrobial agents [8,9].

Numerous studies related to the conversion of glycosides into their respective aglycone moieties using different routes have been reported. Aglycone compounds are significant, considering their effective therapeutic activities. Being lower-molecular-weight compounds, aglycones are easily absorbed through the gastrointestinal tract [10]. After removing sugar moieties from isoflavone glycosides (daidzin, genistin), highly significant isoflavone aglycones such as daidzein and genistein can be generated. Usually, chemical (acid, alkali, etc.) and biological methods (enzymes and microbes) are employed to extract aglycone compounds from conjugated glycosides, albeit with several advantages and disadvantages. Although a chemical process offers advantages with respect to cost and a faster rate of reaction, production of undesired inhibitor compounds because of a lack of specificity toward the substrate makes it unsuitable for application [11]. The hydrolysis of soybean substrates using acids results in the formation of genotoxic compounds, hydroxymethylfurfural and ethoxymethylfurfural, utilizing constituent oligosaccharides [12]. On the other hand, biological methods employing  $\beta$ -glucosidase enzymes and microbial cells [13–16] for the production of aglycones have issues of stability, production cost, and the generation of mixtures of several end products. Therefore, searching for a sustainable and proficient option is crucial for the conversion of glycoside into aglycone compounds.

Regarding this concern, rather than using traditional methods, attention has been paid toward the development of a magnetic acid-functionalized nanocatalyst that possesses catalytic properties and can be easily recovered from the reaction mixture because of its magnetic characteristic [17,18]. Several studies have been reported on the use of various nanobio-catalysts in the pretreatment of different biomass materials [19,20]. Peña et al. [21] used different acid-functionalized magnetic nanocatalysts for cellobiose hydrolysis and among the used nanomaterials, alkylsulfonic acid-functionalized nanomaterial exhibited higher efficiency with 78% cellobiose conversion. In addition, carbon-based nanomaterials functionalized with sulfonic acids have been studied for cellobiose hydrolysis, which generated monomeric glucose with 84% conversion efficiency [22]. Fe-based nanomaterials have also been known to possess exceptional enzyme-mimicking properties, along with a magnetic property. Considering all these aspects, we attempted to mimic the  $\beta$ -glucosidase activity of an acid-functionalized cobalt ferrite alkyl sulfonic acid (CoFe<sub>2</sub>O<sub>4</sub>-Si-ASA) nanocatalyst in an effective manner to hydrolyze the glycosidic linkages in soybean-derived glycoside moieties to obtain aglycones. In this study, a CoFe<sub>2</sub>O<sub>4</sub>-Si-ASA nanocatalyst was prepared and the hydrolytic efficiency was assessed for hydrolysis of glycosides with the aim of developing a simple, sustainable, and ecofriendly approach for the generation of aglycone compounds from glycoside conjugates. An unexplored acid-functionalized nanocatalyst was used for the conversion of soybean-derived glycosides into aglycones, as demonstrated in Figure 1.

The hydrolysis of soybean-extracted glycosides was conducted using a magnetic CoFe<sub>2</sub>O<sub>4</sub>-Si-ASA nanocatalyst and compared with enzymatic hydrolysis. For enzymatic hydrolysis,  $\beta$ -glucosidase produced by *Fusarium verticillioides* was used in this study. *F. verticillioides* has been reported earlier to produce cellulases under submerged fermentation conditions for application in cellulose hydrolysis [23]. In the current investigation, we optimized the solid-state fermentation conditions for cellulase production to obtain enzymes in concentrated form with higher activities using *F. verticillioides*. To accomplish our objectives, optimization studies for hydrolysis of soybean-derived isoflavone glycoside using an acid-functionalized CoFe<sub>2</sub>O<sub>4</sub>-Si-ASA magnetic nanocatalyst were conducted to obtain higher titers of aglycones. To date, microbial enzymes have been used for the generation of aglycone compounds, which is a costlier process than using a nanocatalyst. To our knowl-

edge, this is the first study on the application of nanocatalyst to generate aglycones from glycosides. The application of this nanomaterial-assisted approach of generating aglycone moieties from plant glycosides will have abundant prospectives in the therapeutic industry.

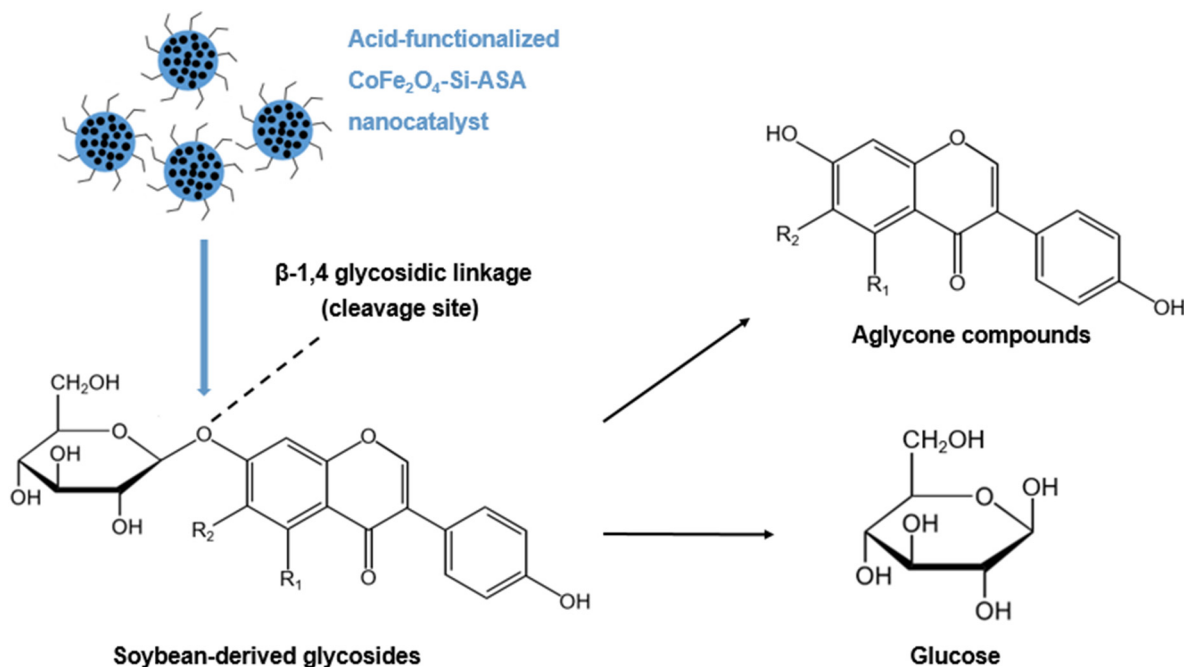


**Figure 1.** Illustrative representation of CoFe<sub>2</sub>O<sub>4</sub>-Si-ASA nanocatalyst-mediated conversion of soybean-derived glycosides into aglycones, i.e., daidzein and genistein.

## 2. Materials and Methods

### 2.1. Chemicals

Cellulose, p-nitrophenyl-β-D-glucopyranoside (p-NPG), isoflavone glycoside standards (genistin and daidzin), and their aglycone counterparts (genistein and daidzein) were purchased from Sigma-Aldrich (St. Louis, MO, USA). Soybean flour and wheat bran were procured from the local market. Ammonium hydroxide, isopropanol, and toluene were purchased from Fisher Scientific (Pittsburgh, PA, USA). 3-mercaptopropyltrimethoxysilane (MPTMS), 4-(triethoxysilyl)-butyronitrile (98%), diethylamine (99%), methylamine (40%), sodium dodecyl sulfate, and tetraethylorthosilicate (TEOS) (99.999%) were purchased from Sigma-Aldrich. Iron (II) chloride tetrahydrate (FeCl<sub>2</sub>·4H<sub>2</sub>O) (97%), and cobalt (II) chloride hexahydrate (CoCl<sub>2</sub>·6H<sub>2</sub>O) (97%) were purchased from Junsei Chemical Co. Ltd., Tokyo, Japan. All other chemicals and reagents used in this study were purchased locally.

### 2.2. Synthesis and Functionalization of Nanoparticles

The synthesis of cobalt ferrite (CoFe<sub>2</sub>O<sub>4</sub>) nanoparticles (NPs) was carried out using the method described by Wang et al. [24] with slight modifications. Furthermore, silica coating and acid functionalization of the synthesized magnetic CoFe<sub>2</sub>O<sub>4</sub> NPs were performed as per the method described by Ingle et al. [25].

#### 2.2.1. Synthesis of Magnetic CoFe<sub>2</sub>O<sub>4</sub> Nanoparticles (CoFe<sub>2</sub>O<sub>4</sub> MNPs)

For the synthesis of CoFe<sub>2</sub>O<sub>4</sub> NPs, 10 mM of CoCl<sub>2</sub>·6H<sub>2</sub>O was mixed with 20 mM of FeCl<sub>2</sub>·4H<sub>2</sub>O solution to make the volume 250 mL of aqueous solution, and then 50 mM sodium dodecyl sulfate was added to the mixture. This solution mixture was kept for stirring initially at 30 °C for half an hour before elevating the temperature to 70 °C. In the meantime, another solution (500 mL) was prepared with 75 mL of methylamine (40% w/w) and distilled water, which was further heated at 70 °C. Finally, both solutions were mixed and stirred for 3 h. The synthesized NPs were separated magnetically and washed thrice

with distilled water followed by ethanol. The isolated MNPs were dried in a hot-air oven at 60 °C for characterization studies.

### 2.2.2. Synthesis of Silica Coated CoFe<sub>2</sub>O<sub>4</sub> Nanoparticles (CoFe<sub>2</sub>O<sub>4</sub>-Si MNPs)

The silica coating of CoFe<sub>2</sub>O<sub>4</sub> MNPs was conducted by combining the process described by Rajkumari et al. [26] and Peña et al. [21]. The synthesized CoFe<sub>2</sub>O<sub>4</sub> MNPs were dispersed in ethanol and sonicated for 15–20 min. Then 25 mL of the ethanol-dispersed CoFe<sub>2</sub>O<sub>4</sub> MNPs solution was added to 430 mL of isopropanol and 20 mL of distilled water. This solution was further sonicated for 15 min and then 50 mL of concentrated NH<sub>4</sub>OH was added to the mixture. The solution of TEOS/isopropanol (1:40) was added dropwise to the earlier solution and sonicated with stirring for 4 h. The synthesized NPs were separated magnetically, washed with distilled water, and finally dried in a hot-air oven at 80 °C for 24 h.

### 2.2.3. Acid Functionalization of CoFe<sub>2</sub>O<sub>4</sub>-Si MNPs Using Alkylsulfonic Acid (CoFe<sub>2</sub>O<sub>4</sub>-Si-ASA)

An acid-functionalized catalyst, CoFe<sub>2</sub>O<sub>4</sub>-Si-ASA, was synthesized by functionalizing silica-coated CoFe<sub>2</sub>O<sub>4</sub> MNPs with ASA by following the method reported by Wang et al. [24] with slight variations. For the preparation of acid functionalized CoFe<sub>2</sub>O<sub>4</sub>-Si nanocatalyst, a solution mixture containing MPTMS (5.0 mL), ethanol (50 mL), and distilled water (45 mL) was prepared and then 0.5 g of CoFe<sub>2</sub>O<sub>4</sub>-Si MNPs was added. This solution mixture was sonicated for 30 min and further kept overnight for stirring at 70 °C. CoFe<sub>2</sub>O<sub>4</sub>-Si MNPs with attached thiol groups were collected magnetically and washed thrice with distilled water. A solution of 50% H<sub>2</sub>O<sub>2</sub> (30 mL), distilled water (30 mL), and methanol (30 mL) was added to the recovered thiol-attached CoFe<sub>2</sub>O<sub>4</sub>-Si MNPs and the mixture was kept at room temperature for oxidation of thiol to sulfonic acid groups. After oxidation, the formed acid-functionalized CoFe<sub>2</sub>O<sub>4</sub>-Si-ASA nanocatalyst was recovered magnetically and washed with distilled water thrice. The synthesized acid-functionalized CoFe<sub>2</sub>O<sub>4</sub>-Si-ASA nanocatalyst was further reacidified with 3 M H<sub>2</sub>SO<sub>4</sub> (25 mL), washed two or three times with distilled water, and finally dried in a hot-air oven at 80 °C for 24 h. Furthermore, the synthesis of all these nanomaterials was validated by characterization studies.

### 2.3. Characterization of Synthesized Nanoparticles

To study the surface morphology of the synthesized NPs, scanning electron microscopy (SEM, LEO-1530) analysis was conducted. The samples were prepared by platinum coating and images were recorded at an accelerating voltage of 3 kV. Furthermore, the sizes of the synthesized NPs were estimated using transmission electron microscopy (TEM, Carl Zeiss, Libra 120, Jena, Germany) at a voltage of 120 kV. For TEM analysis, samples were prepared by dispersing the synthesized NPs in water, which was then sonicated for about 5–10 min. These dispersed samples were further adsorbed onto 200-mesh copper grids for 30–60 s at room temperature and then viewed by TEM. To determine the elemental composition, the synthesized NPs were further analyzed using energy dispersive X-ray spectroscopy (EDX, Thermo Fisher Scientific, Waltham, MA, USA). Fourier transform-infrared spectroscopy (FTIR) analysis was used to examine the absorption peaks and functional groups present on the synthesized nanomaterials. FTIR analysis of the synthesized NPs was carried out using an IR200 spectrometer (Thermo Fisher Scientific) in a wavenumber range of 400–4000 cm<sup>-1</sup> by following the KBr pellet method as reported earlier [23]. X-ray diffraction (XRD) was carried out to determine the degree of cellulose crystallinity for raw and pretreated corncob biomass using a high-power X-ray diffractometer (model: JP/SmartLab, 9 kW). Samples were analyzed from 2θ = 5 to 70° at a scanning speed of 3°/min [23].

### 2.4. Microbial Strain, Medium, and β-Glucosidase Enzyme Production

In this study, the previously isolated fungal strain, *Fusarium verticillioides* (Accession no. PRJNA664836), was used for cellulase enzyme, particularly β-glucosidase, production.

The strain was regularly maintained and sub-cultured every three months on potato dextrose agar (PDA) slants under optimized growth conditions as reported earlier [23]. The method for the medium preparation and its composition used in this study was similar as reported earlier [16]. The response surface methodology-optimized basal medium (RSM-BM) consisted of (per L):  $\text{KH}_2\text{PO}_4$  (1.0 g),  $\text{CaCl}_2$  (0.15 g), urea (0.60 g),  $(\text{NH}_4)_2\text{SO}_4$  (0.50 g), yeast extract (0.15 g), peptone (0.45 g),  $\text{MgSO}_4 \cdot 7\text{H}_2\text{O}$  (0.15 g),  $\text{FeSO}_4 \cdot 7\text{H}_2\text{O}$  (0.0075 g),  $\text{MnSO}_4 \cdot 7\text{H}_2\text{O}$  (0.0024 g),  $\text{ZnSO}_4 \cdot 7\text{H}_2\text{O}$  (0.0021 g),  $\text{CoCl}_2$  (0.003 g), and Tween 80 (1.0 mL). The cellulase production experiments were conducted under solid-state fermentation conditions using the *F. verticillioides* fungal strain.

Solid-state fermentation was carried out in 250 mL Erlenmeyer flasks containing 4 g of wheat bran, 1 g of cellulose, and 8 mL of production medium (RSM-BM) to moisten the substrate. The spore suspension from the sporulated fungal slant was prepared using saline water containing triton X-100 (0.1% v/v). The flasks were inoculated with spores (about  $10^7$ – $10^8$ ) derived from fungal strain grown on PDA slants and incubated at 28 °C under static conditions. The inoculated flasks were extracted by adding 50 mL of sodium citrate buffer (50 mM, pH 4.5) after every 2-day interval. For enzyme extraction, flasks were incubated at 37 °C with shaking at 200 rpm for 2 h. The extracted broth was centrifuged at 8000 rpm for 10 min and the supernatant was collected. All supernatant samples were analyzed to determine extracellular  $\beta$ -glucosidase activity and protein concentration. The extracted enzyme supernatant was further used for the hydrolysis of soybean-derived glycosides.

#### 2.5. Hydrolysis of Soybean-Derived Glycosides Using Acid-Functionalized $\text{CoFe}_2\text{O}_4$ -Si-ASA Nanocatalyst and $\beta$ -Glucosidase Enzyme

The soybean flour was extracted using methanol, as reported previously [16] with slight modifications. For the glycoside extraction experiment, soybean flour was defatted with three volumes of *n*-hexane by stirring for 30 min at 30 °C, centrifuging at 10,000 rpm for 20 min, and air drying. The defatted soybean flour (10 g) was further treated with 50 mL of methanol (80%), stirring for 2 h at 80 °C and centrifuging at 10,000 rpm for 10 min to obtain the extract containing glycosides.

To evaluate and compare the catalytic efficiency of the acid-functionalized  $\text{CoFe}_2\text{O}_4$ -Si-ASA nanocatalyst with  $\beta$ -glucosidase enzymes, this soybean extract containing glycosides was hydrolyzed using a  $\text{CoFe}_2\text{O}_4$ -Si-ASA nanocatalyst and  $\beta$ -glucosidase enzymes derived from *F. verticillioides* in two different flasks. In the case of hydrolysis using acid-functionalized  $\text{CoFe}_2\text{O}_4$ -Si-ASA nanocatalyst, different concentrations of NPs (50, 150, 250, 350, and 450 mg per g of substrate) were used for hydrolysis of soy-flour extract. The initial optimization studies for soybean-derived glycoside hydrolysis were performed using different concentrations of  $\text{CoFe}_2\text{O}_4$ -Si-ASA nanocatalyst at 80 °C. After optimizing the concentration of the nanocatalyst, the hydrolysis performance was checked at higher temperature and pressure conditions, i.e., at 120 °C and 15 psi pressure, respectively, for 1 h. After hydrolysis, the samples were analyzed to determine the content of aglycones using high-performance liquid chromatography (HPLC) analysis.

Furthermore, to assess the catalytic performance of the  $\text{CoFe}_2\text{O}_4$ -Si-ASA nanocatalyst, in-house-generated  $\beta$ -glucosidase enzymes were used for comparative glycoside hydrolysis. For enzymatic hydrolysis, 10 mL of soybean-flour extract was hydrolyzed with 5.0 IU of  $\beta$ -glucosidase at 60 °C for different time intervals as optimized previously [16]. The obtained samples after hydrolysis were dried under vacuum and resuspended in methanol (1 mL) prior to HPLC analysis. The reaction mixture without  $\text{CoFe}_2\text{O}_4$ -Si-ASA nanocatalyst/enzyme was used as control.

#### 2.6. Recovery and Reuse of $\text{CoFe}_2\text{O}_4$ -Si-ASA Nanocatalyst for Hydrolysis Experiments

After the first hydrolysis reaction, the acid-functionalized  $\text{CoFe}_2\text{O}_4$ -Si-ASA MNPs were easily separated by applying a magnetic field and the remaining liquid hydrolysate was collected to analyze the concentration of aglycones (daidzein and genistein) formed

after hydrolysis. Hence, the recovered NPs were further washed two to three times with distilled water and dried at 70 °C in a hot-air oven overnight and reused in the subsequent hydrolysis reaction. The recovered CoFe<sub>2</sub>O<sub>4</sub>-Si-ASA MNPs after the first cycle of hydrolysis were reused in the next cycle of hydrolysis. All these hydrolysis experiments using reused MNPs were performed at similar conditions to those used for optimization studies (at 80 °C for 3 h), as mentioned in the above Section 2.5.

### 2.7. Analytical Methods

To evaluate the acidity of the synthesized nanocatalyst, an ion-exchange titration method was used, as reported earlier [27]. To remove the hydronium ions from the nanocatalyst, 50 mg of catalyst was added to 20 mL of a sodium chloride/tetramethylammonium chloride (2 M). This test solution was sonicated, kept static at room temperature overnight, and then titrated to neutrality with a 10 mM NaOH solution. The extracted solid-state enzymes and CoFe<sub>2</sub>O<sub>4</sub>-Si-ASA nanocatalyst were tested for β-glucosidase-mimicking activity using a *p*-NPG substrate, as reported earlier [16]. The enzyme supernatant was analyzed to determine protein concentration using the bicinchoninic acid assay method [28]. The concentration of glycosides (daidzin and genistin) in soybean flour and the obtained aglycones (daidzein and genistein) in the hydrolysate were determined using reverse phase HPLC (YL 9100, Younglin Inc., Anyang, Korea), as reported earlier [16]. HPLC analysis was conducted with a YL 9100 system and an Eclipse plus C18 (4.6 mm × 250 mm, 5 μm) column at 260 nm for 60 min and the column temperature was set at 35 °C [29]. An isocratic elution was performed using an acetonitrile (10%, *v/v*) mobile phase at a flow rate of 0.3 mL/min. The unknown amounts of glycosides and aglycones were determined by correlating with standards. For further authentication of the glycosides and aglycones present in the control and hydrolysate samples, the mass spectrum was determined by LC/MS (maXis 4G, Bruker Biosciences, Billerica, MA, USA) using an ESI detector.

## 3. Results and Discussion

### 3.1. Synthesis and Characterization of All Synthesized Nanoparticles

All three MNPs, i.e., CoFe<sub>2</sub>O<sub>4</sub>, CoFe<sub>2</sub>O<sub>4</sub>-Si, and acid-functionalized CoFe<sub>2</sub>O<sub>4</sub>-Si-ASA, used in this study were prepared as mentioned above (Materials and Methods Section 2.2). To confirm the synthesis of all three MNPs, characterization studies were conducted using SEM, TEM, EDX, FTIR, and XRD analyses.

To determine the surface morphology and shape of all three synthesized nanomaterials, the CoFe<sub>2</sub>O<sub>4</sub>, CoFe<sub>2</sub>O<sub>4</sub>-Si, and acid-functionalized CoFe<sub>2</sub>O<sub>4</sub>-Si-ASA were subjected to SEM analysis. All three MNPs were observed to be spherical and uniform in shape (Figures S1A,B and 2A). Furthermore, TEM analysis confirmed that the synthesis of all MNPs was successful from their nano-sizes ranging from 5–25 nm. The diameters of CoFe<sub>2</sub>O<sub>4</sub>, CoFe<sub>2</sub>O<sub>4</sub>-Si, and acid-functionalized CoFe<sub>2</sub>O<sub>4</sub>-Si-ASA were recorded to be in the range of 7.74–25.2, 5.07–4.11, and 5.2–12.2 nm (as presented in Figure S1C,D and Figure 2B), respectively. Among all three MNPs, acid-functionalized CoFe<sub>2</sub>O<sub>4</sub>-Si-ASA (Figure 2B) and CoFe<sub>2</sub>O<sub>4</sub> NPs (Figure S1C) were well dispersed, whereas the silica-coated CoFe<sub>2</sub>O<sub>4</sub>-Si NPs were observed to be agglomerated (Figure S1D).

EDX analysis is usually used to determine the elemental composition of any material. Furthermore, the elemental composition of all three MNPs characterized using EDX confirmed the occurrence of metal constituents, oxygen, carbon, and other components in each nanomaterial. As shown in Figure S2, strong signals for specific metals (Fe: 0.64 eV; Co: 0.70 eV; Si: 0.18 eV; S: 0.24 eV; C: 0.27 eV, and O: 0.51 eV) confirmed the formation of the desired nanomaterials. The details of the elemental composition of all nanomaterials are given in Table 1. The EDX analysis exhibited 15.13 wt% of Fe and 23.47 wt% of Co in case of the CoFe<sub>2</sub>O<sub>4</sub> MNPs. The presence of elemental Fe and Co in major amounts assured us that the synthesized NPs are CoFe<sub>2</sub>O<sub>4</sub> MNPs. Besides this, the peaks corresponding to the element Si were observed in the cases of both silica-coated CoFe<sub>2</sub>O<sub>4</sub>-Si and acid-functionalized CoFe<sub>2</sub>O<sub>4</sub>-Si-ASA MNPs designating the effective surface amendment by silica on bare

$\text{CoFe}_2\text{O}_4$  MNPs [30]. Furthermore, a substantial occurrence of sulfur (S) in the case of  $\text{CoFe}_2\text{O}_4\text{-Si-ASA}$  (5.05 wt%) indicated the strong functionalization of acid on  $\text{CoFe}_2\text{O}_4\text{-Si}$  MNPs. In the case of acid-functionalized  $\text{CoFe}_2\text{O}_4\text{-Si-ASA}$  MNPs, a large amount of C was detected with respect to the S element, specifying the probable loss of the sulfonic acid groups during the MNP synthesis process. The XRD spectra of the  $\text{CoFe}_2\text{O}_4\text{-Si-ASA}$  MNPs are shown in Figure S3. The obtained XRD spectrum for  $\text{CoFe}_2\text{O}_4\text{-Si-ASA}$  MNPs agrees well with reported studies [21]. The XRD pattern for the  $\text{CoFe}_2\text{O}_4\text{-Si-ASA}$  MNPs shows all the respective signals for the  $\text{CoFe}_2\text{O}_4$  crystals; this spectrum has an additional peak between  $20$  and  $30^\circ$  ( $2\theta$ ), which is associated with amorphous silica. The size of the  $\text{CoFe}_2\text{O}_4\text{-Si-ASA}$  MNPs was calculated as  $21.6$  nm, which seems to be larger than those obtained with TEM. The larger sizes calculated from the XRD patterns could be due to the possible aggregation of MNPs. In addition, the magnetic behavior of  $\text{CoFe}_2\text{O}_4$  MNPs was confirmed by providing a magnetic field, as shown in Figure S4.

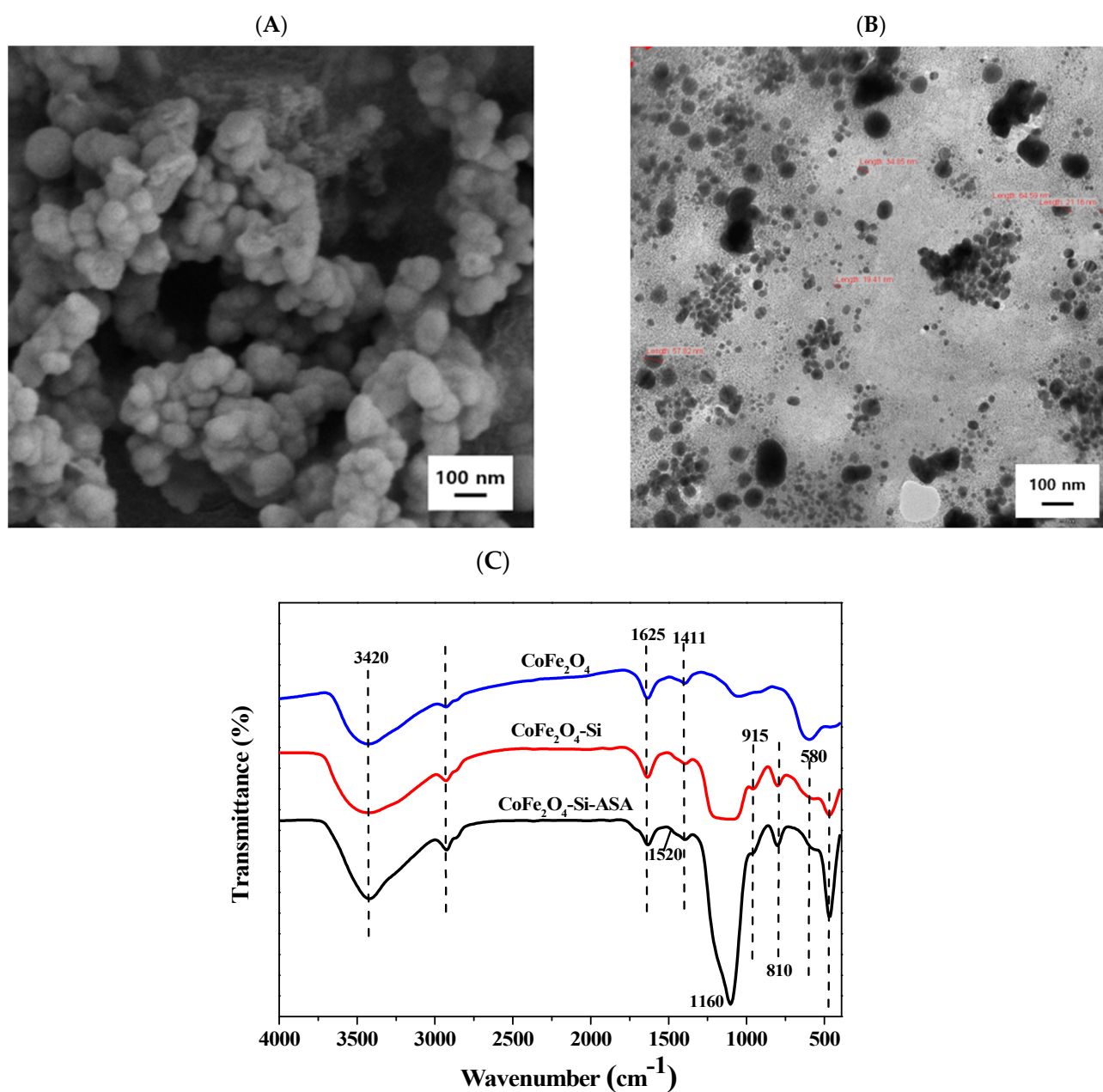


**Figure 2.** Characterization of the synthesized  $\text{CoFe}_2\text{O}_4\text{-Si-ASA}$  nanocatalyst using (A) SEM, (B) TEM, and (C) FTIR analyses.

**Table 1.** Elemental composition of nanoparticles used in this study.

Synthesized Nanoparticles	Atomic Weight Percentage (%) <sup>a</sup>						Acid Capacity (mM H <sup>+</sup> /g) <sup>b</sup>
	C	O	Fe	Co	Si	S	
CoFe <sub>2</sub> O <sub>4</sub>	34.19	27.20	15.13	23.47	-	-	-
CoFe <sub>2</sub> O <sub>4</sub> -Si	37.16	53.01	1.13	1.12	7.59	-	-
CoFe <sub>2</sub> O <sub>4</sub> -Si-ASA	51.23	38.69	0.18	0.21	4.64	5.05	0.92

<sup>a</sup> data obtained from EDX analysis. <sup>b</sup> calculated using titration method

FTIR analysis is generally used to identify the functional groups present in the experimental samples. Figure 2C depicts the FTIR spectra of all three synthesized MNPs, CoFe<sub>2</sub>O<sub>4</sub>, CoFe<sub>2</sub>O<sub>4</sub>-Si, and acid-functionalized CoFe<sub>2</sub>O<sub>4</sub>-Si-ASA. As shown in Figure 2C, the significant peak was detected in the wavelength range of 520–560 cm<sup>-1</sup> in all three MNPs assigning to the stretching of the Fe-O bond [31], which is one of the confirmatory features of CoFe<sub>2</sub>O<sub>4</sub>-MNPs. The common absorption peaks at wavelengths of 800 and 910 cm<sup>-1</sup>, ascribed to the stretching vibrations of the Si-O-Si and Si-O-H groups, appeared only in CoFe<sub>2</sub>O<sub>4</sub>-Si and acid-functionalized CoFe<sub>2</sub>O<sub>4</sub>-Si-ASA [24]. These peaks were not observed in CoFe<sub>2</sub>O<sub>4</sub> MNPs, specifying the surface coating of silica in the case of CoFe<sub>2</sub>O<sub>4</sub>-Si and acid-functionalized CoFe<sub>2</sub>O<sub>4</sub>-Si-ASA MNPs only. Similarly, stretching vibrations at 1160 and 1380 cm<sup>-1</sup>, assigned to Si-O and O=S=O stretching vibrations, were observed in the spectra of both CoFe<sub>2</sub>O<sub>4</sub>-Si and acid-functionalized CoFe<sub>2</sub>O<sub>4</sub>-Si-ASA samples [32]. The presence of peaks at a wavelength of about 1420 cm<sup>-1</sup>, attributed to undissociated SO<sub>3</sub>H groups, was found only in acid-functionalized CoFe<sub>2</sub>O<sub>4</sub>-Si-ASA MNPs [33], further confirming the effective functionalization of acids on silica-coated MNPs. The obtained FTIR spectra for all three MNPs indicated common peaks at the wavelengths of 3420, 2810, and 1625 cm<sup>-1</sup>, which correspond to the stretching vibrations of the O-H and C-H groups, respectively [21]. The results obtained from FTIR analysis revealed the presence of all of the expected functional groups in the case of all three synthesized MNPs.

The overall results obtained after characterizing all these materials revealed that strong magnetic CoFe<sub>2</sub>O<sub>4</sub> NPs were synthesized and appropriately coated with silica, which was confirmed by the FTIR and EDX analyses. Similarly, TEM analysis confirmed that the synthesis of all NPs was successful from their nano-sizes in the range of 5–25 nm. Thus, after confirming the synthesis of all three MNPs through characterization studies, acid-functionalized CoFe<sub>2</sub>O<sub>4</sub>-Si-ASA nanocatalyst was further evaluated for its hydrolytic activity to generate therapeutic aglycone compounds from soybean-derived glycosides.

### 3.2. $\beta$ -Glucosidase Enzyme Production by Solid-State Fermentation

The isolated fungal strain, *F. verticillioides* was assessed for production of extracellular  $\beta$ -glucosidase enzyme in flasks using RSM-BM [16] containing wheat bran (4.0 g) and cellulose (1.0 g) substrates under solid-state fermentation conditions. As presented in Table 2, the optimized RSM-BM containing wheat bran (2.5%) and cellulose (1%) exhibited maximum  $\beta$ -glucosidase activity ( $1.959 \pm 0.098$  IU/g) under solid-state fermentation conditions. Previously, we have reported the production of cellulases under submerged fermentation conditions, which exhibited the highest activity of  $\beta$ -glucosidase ( $2.91 \pm 0.12$  IU/mL) on the 8<sup>th</sup> day of fermentation [23]. As enzymes produced under submerged fermentation conditions are usually in the diluted form, we attempted to produce enzymes in the concentrated form using solid-state fermentation in this study. As shown in Table 2, the higher enzyme activities were obtained on the 6<sup>th</sup> day of fermentation, which reduced the fermentation time and increased  $\beta$ -glucosidase activities as compared to previously reported enzyme activities using submerged fermentation [23].

**Table 2.** Determination of  $\beta$ -glucosidase activities produced by *Fusarium verticillioides* under solid-state fermentation conditions.

Fermentation Time (Days)	$\beta$ -Glucosidase (IU/g)	Protein (mg/g)
2nd day	0.453 $\pm$ 0.021	0.153 $\pm$ 0.0082
4th day	1.858 $\pm$ 0.101	0.858 $\pm$ 0.049
6th day	1.959 $\pm$ 0.098	0.895 $\pm$ 0.052
8th day	2.052 $\pm$ 0.111	0.782 $\pm$ 0.043

A fermentation experiment was carried out at 28 °C under solid-state conditions in the fermentation medium containing wheat bran (4 g) and cellulose (1 g) substrates. The standard deviation values represented in the table are derived from the experiment performed in triplicate.

There are very few studies conducted on the production of cellulases with such higher activities under solid-state fermentation using *Fusarium* sp. Ramanathan et al. [34] reported cellulase activities produced by the *F. oxysporum* strain under submerged fermentation conditions, which exhibited  $\beta$ -glucosidase activities of 1.784 IU/mL, along with endoglucanase (1.921 IU/mL) and exoglucanase (1.342 IU/mL) activities. The *F. verticillioides* strain demonstrated both  $\beta$ -glucosidase (0.39 IU/mL) and endoglucanase (6.5 IU/mL) enzyme activities using gamba grass as a substrate [35], which are lower than those obtained in the present study. Hence,  $\beta$ -glucosidase produced by *F. verticillioides* was further used as control in the conversion of soybean-derived glycosides.

### 3.3. Comparative Studies on Hydrolysis of Soybean-Derived Glycosides Using CoFe<sub>2</sub>O<sub>4</sub>-Si-ASA Nanocatalyst and $\beta$ -Glucosidase Enzyme

Glycosides such as daidzin and genistin reveal medicinal properties only when processed into their aglycone forms, i.e., daidzein and genistein, respectively [36]. Hence, it is practical to generate daidzein and genistein in bulk amounts from glycosides through a hydrolysis reaction by breaking down  $\beta$ -glycosidic linkages. Traditionally,  $\beta$ -glucosidase enzymes have been used for the generation of aglycones, which is not a viable option considering the high cost of enzyme production. Nowadays, enzyme-mimicking nanomaterials have been employed for several applications such as biomass hydrolysis. In the present study, we have applied  $\beta$ -glucosidase-mimicking CoFe<sub>2</sub>O<sub>4</sub>-Si-ASA nanocatalyst to generate daidzein and genistein from soybean-derived glycosides and further compared their catalytic efficiencies with  $\beta$ -glucosidase enzyme during hydrolysis reaction.

#### 3.3.1. Hydrolysis of Soybean-Derived Glycosides Using CoFe<sub>2</sub>O<sub>4</sub>-Si-ASA Nanocatalyst

First, the synthesized CoFe<sub>2</sub>O<sub>4</sub>-Si-ASA nanocatalyst was tested for its catalytic ability in converting soybean glycosides into aglycones. As mentioned above in the Materials and Methods Section 2.5, optimization studies for hydrolysis of soybean-extracted glycosides were carried out at 80 °C using various concentrations of nanocatalyst (i.e., 50, 150, 250, 350, and 450 mg/g of substrate used) and samples were taken after every hour. The maximum conversions of glycosides were obtained after 3 h of hydrolysis reaction and there was no further increase in glycoside conversion observed. Hence, the hydrolysis reaction was stopped after 3 h of hydrolysis (data not shown). As the amount of nanocatalyst used in the hydrolysis reaction majorly affects the activity, different concentrations of CoFe<sub>2</sub>O<sub>4</sub>-Si-ASA were verified as depicted in Figure 3. At lower concentration (i.e., 50 mg/g), the nanocatalyst showed very slight conversion. With increasing quantities of nanocatalyst, the hydrolysis caused by the acidic sulfonic groups seemed to be activated and ultimately resulted in a higher conversion of glycosides. As illustrated in Figure 3, the hydrolysis profile exhibited that the rate of hydrolysis and the generation of daidzein and genistein compounds was influenced by the concentrations of the CoFe<sub>2</sub>O<sub>4</sub>-Si-ASA nanocatalyst used. An increase in the concentration of nanocatalyst also upturns the generation of aglycones after hydrolyzing glycosides, which was examined by HPLC analysis. In the case of using a 350 mg/g concentration of CoFe<sub>2</sub>O<sub>4</sub>-Si-ASA nanocatalyst, the maximum 8.91 g/L of daidzein and 12 g/L of genistein was achieved from 15.1 g/L daidzin and

19.3 g/L genistin with the conversion efficiency of 59% and 62.2%, respectively, which were relatively higher than the other concentrations of nanocatalyst used. Thus, for further hydrolysis experiments, the optimized concentration of nanocatalyst (350 mg/g) was used.

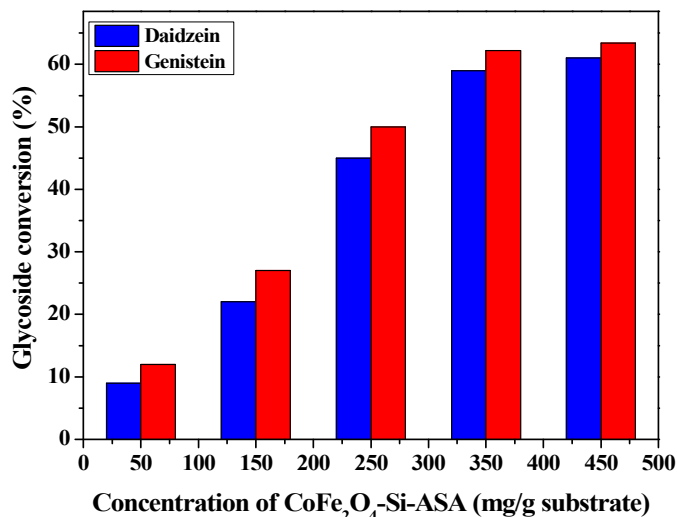


**Figure 3.** Hydrolysis of soybean-derived glycosides into aglycones using different concentrations of CoFe<sub>2</sub>O<sub>4</sub>-Si-ASA nanocatalyst at 80 °C for 3 h.

Moreover, to check the effect of higher temperature and pressure conditions on the catalytic performance of the CoFe<sub>2</sub>O<sub>4</sub>-Si-ASA nanocatalyst, hydrolysis experiments were carried out at 120 °C and 15 psi pressure for 1 h. As presented in Table 3, the hydrolysis reaction performed at 120 °C and 15 psi pressure generated the maximum 10.7 g/L of daidzein and 13.7 g/L genistein with conversion efficiencies of 69.2% and 73.2%, respectively. This reaction condition exhibited 10–11% enhancement in the generation of aglycone compounds as compared to the aglycones produced during the hydrolysis reaction at 80 °C (as compared in Table 3). Although a slight improvement was observed in the hydrolytic performance of the nanocatalyst at higher temperature and pressure conditions, the hydrolysis reaction at 80 °C is preferred, concerning the lower energy requirement, no formation of inhibitor compounds, and better recyclability of the nanocatalyst. Thus, further hydrolysis experiments employing the nanocatalyst were performed at 80 °C for 3 h.

**Table 3.** Comparative analysis of hydrolytic conversion of soybean-derived glycosides into aglycone compounds using acid-functionalized cobalt ferrite alkyl sulfonic acid (CoFe<sub>2</sub>O<sub>4</sub>-Si-ASA) nanocatalyst and enzyme  $\beta$ -glucosidase.

Catalyst Used	Glycosides (g/L)		Aglycones (g/L)	
	Daidzin	Genistin	Daidzein	Genistein
CoFe <sub>2</sub> O <sub>4</sub> -Si-ASA (80 °C for 3 h)	15.1 ± 0.51	19.3 ± 0.68	8.91 ± 0.45 (59.0%)	12.0 ± 0.48 (62.2%)
CoFe <sub>2</sub> O <sub>4</sub> -Si-ASA (120 °C at 15 psi for 1 h)	15.5 ± 0.68	18.7 ± 0.99	10.7 ± 0.41 (69.2%)	13.7 ± 0.51 (73.3%)
$\beta$ -glucosidase enzyme (60 °C for 2 h)	14.8 ± 0.81	17.9 ± 0.91	12.1 ± 0.72 (81.8%)	15.6 ± 0.62 (87.2%)

The standard deviation values are from three independent experiments.

### 3.3.2. Hydrolysis of Soybean-Derived Glycosides Using $\beta$ -Glucosidase Enzymes

For comparative evaluation,  $\beta$ -glucosidase enzymes produced by *F. verticillioides* were used as biocatalyst for the hydrolysis of soybean-derived glycosides. As demonstrated

in Table 3, the enzymatic hydrolysis of soybean-derived glycosides converted daidzin (14.8 g/L) and genistin (17.9 g/L) into daidzein (12.1 g/L) and genistein (15.6 g/L) with conversion efficiencies of 81.7% and 87.5%, respectively. The application of enzyme exhibited better catalytic ability than the nanocatalyst toward the hydrolysis of soy flour glycosides. There are many studies reported on the production of various aglycone compounds by hydrolyzing soybean-derived isoflavones by  $\beta$ -glucosidases [37–39]. Our present studies exhibited slightly lower conversion efficiencies using nanocatalyst (69–70%) than enzymes (81–87%). However, the higher cost of enzymes, slower rate of reaction, and lower stability, as compared to modern nanocatalyst, constrain their application in the conversion of glycosides into aglycones on a commercial scale. To address these issues, we attempted to employ a magnetic nanocatalyst for the generation of aglycone compounds, which is more sustainable option than biocatalysts.

All the hydrolyzed samples were analyzed using HPLC, demonstrating that the nanocatalyst was active in the conversion of soybean-derived glycosides. The standards of both glycosides (daidzin and genistin) and aglycones (daidzein and genistein) were analyzed using HPLC to determine their retention times and to quantify compounds in control and nanocatalyst-hydrolyzed samples under the conditions mentioned in the above Section 2.7. As shown in Figure 4A, the HPLC profile of the control sample (i.e., unhydrolyzed soybean-derived glycosides) exhibited the peaks for diadzin and genistin accompanied by few other unknown components. In addition, the HPLC profile of the nanocatalyst-hydrolyzed samples designated the presence of diadzein and genistein peaks by matching the retention times with the standards (Figure 4B). Moreover, the peaks observed in the HPLC analysis for both samples were confirmed by LC-MS analysis through the mass spectrum  $[M + H]^+$  peak. The LC-MS analysis authenticated that the obtained compounds were glycosides (daidzin and genistin) in the control samples (Figure 5A) and aglycones (daidzein and genistein) in the nanocatalyst-hydrolyzed samples (Figure 5B) from their molecular weights.

In this study, the conversion efficiencies of the generated diadzein (69.2%) and genistein (73.2%) from soybean-derived glycosides using  $\text{CoFe}_2\text{O}_4$ -Si-ASA nanocatalyst were somewhat lower than enzymatic hydrolysis (as shown in Table 3). Hitherto, there have been no studies reported on the conversion of plant-based glycosides into aglycones using any kind of nanocatalyst. Hence, very limited information is available related to the application of nanomaterials in the conversion of glycoside into aglycones. The overall results obtained in this study were corroborated with some reported studies related to cellobiose hydrolysis into simple glucose sugar molecules using various nanomaterials. Recently, Carlier and Hermans [22] reported higher cellobiose hydrolysis (84%) caused by the catalytic action of carbon nanomaterials functionalized with sulfonic acids, i.e.,  $\text{SO}_3\text{H}$ /reduced graphene oxide catalyst at a temperature of 130 °C in only 2 h. Previously, Peña et al. [21] tested the catalytic efficiency of two different nanomaterials, i.e., acid-functionalized perfluoroalkylsulfonic and alkylsulfonic acid, in the cellobiose hydrolysis at 175 °C, which exhibited 75% and 78% conversion into glucose, respectively. These MNPs were further evaluated for pretreating wheat straw [32] and corn stover [19] at different temperatures, which gave higher hydrolysis as compared to the control. Wang et al. [40] proved the exceptional catalytic abilities of acid-functionalized silica-coated  $\text{Fe}_3\text{O}_4$  MNPs in different catalytic processes. Hence, such nanocatalyst has been used for the pretreatment of various lignocellulosic substrates.

Some of the reported studies, as discussed above, exhibit slightly better conversion efficiencies as compared to our process, but most studies have been conducted under extreme conditions, e.g., higher temperature and pressure. Conversely, our current strategy can be considered as most promising since hydrolysis reaction was conducted under milder conditions. To our knowledge, no studies have been reported on the employment of acid-functionalized nanocatalyst for the production of pharmaceutically significant aglycone compounds. Thus, in this study, we demonstrated a prospective process for the production of aglycones from soybean-derive glycosides using a nanocatalyst.

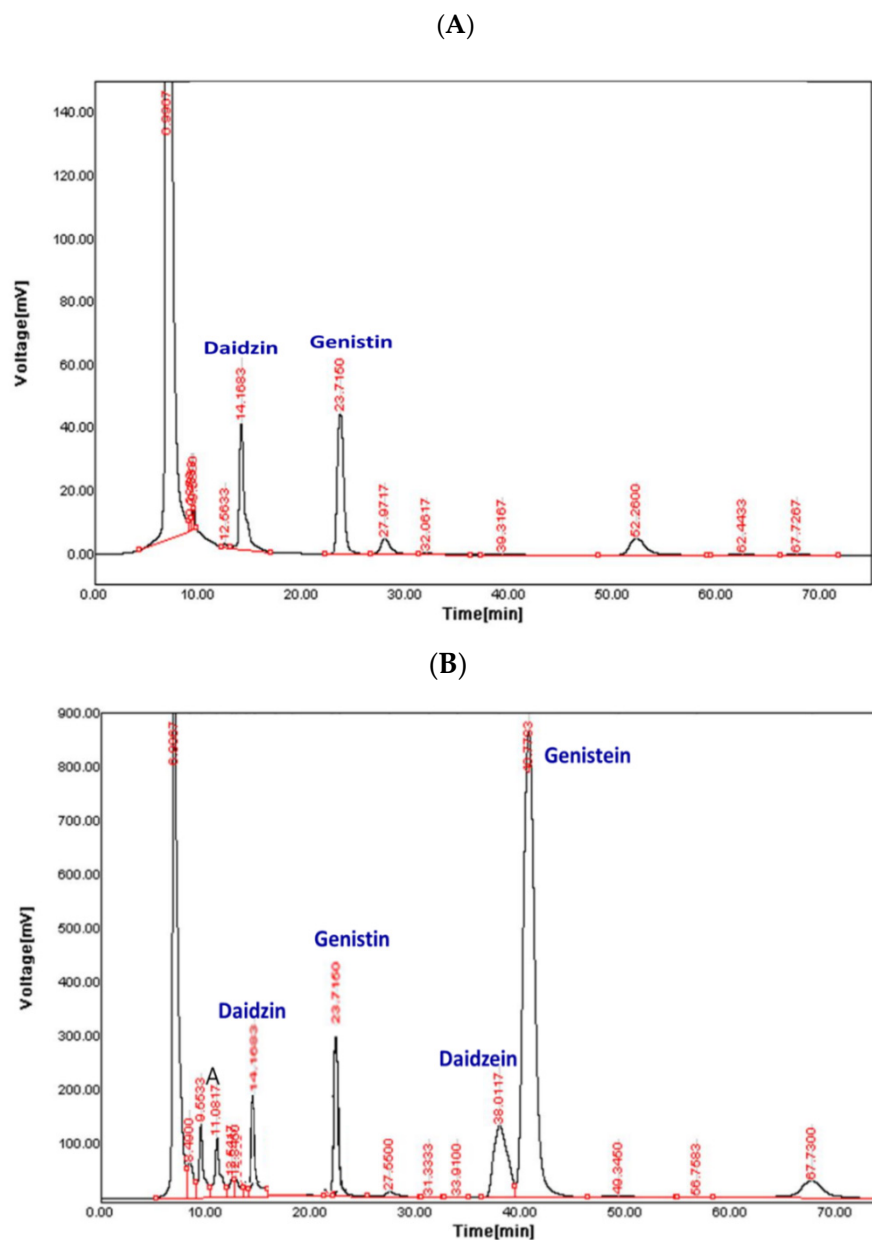


**Figure 4.** HPLC analysis of soybean-derived glycoside components (daidzin and genistin) and their hydrolyzed products containing aglycone (daidzein and genistein) compounds: (A) control (0 h), (B) soy-flour extract after hydrolysis with acid nanocatalyst  $\text{CoFe}_2\text{O}_4\text{-Si-ASA}$  at  $80^\circ\text{C}$  for 3 h.

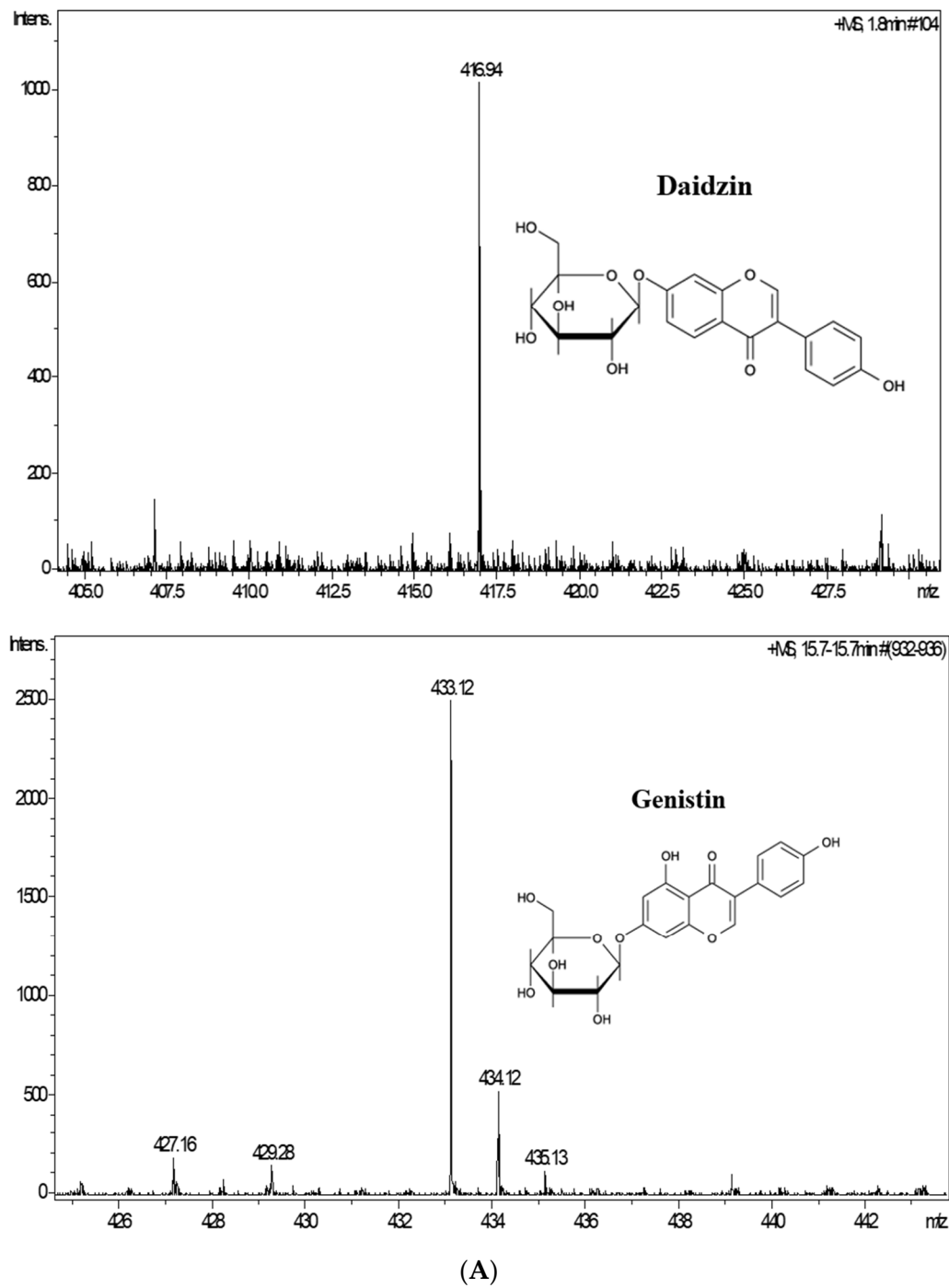
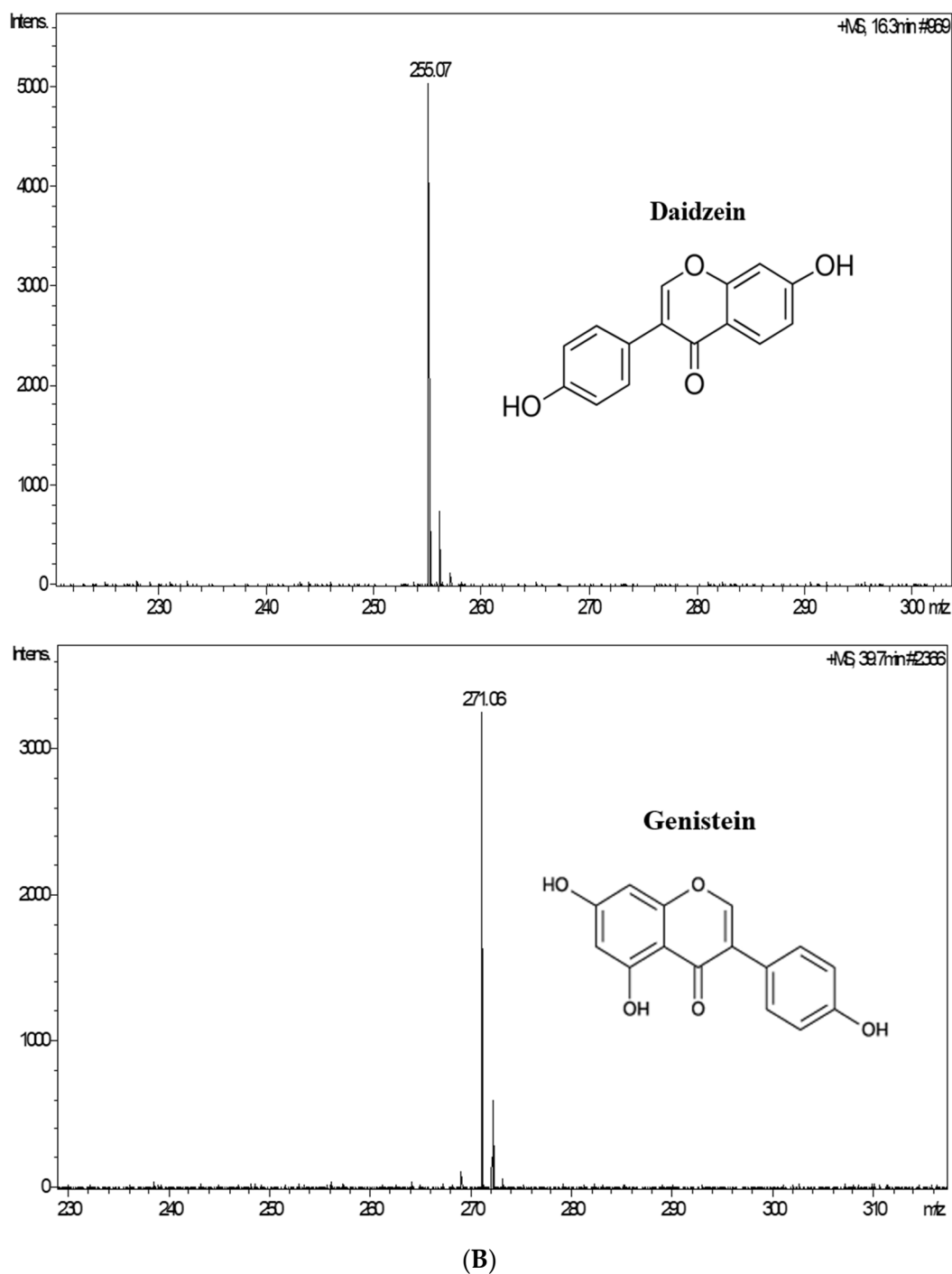


Figure 5. Cont.



**Figure 5.** LC-MS analysis of soybean-derived glycoside components (daidzin and genistin) and their hydrolyzed products containing aglycones (daidzein and genistein) compounds: (A) control (0 h), (B) soy-flour extract after hydrolysis with acid nanocatalyst  $\text{CoFe}_2\text{O}_4\text{-Si-ASA}$  at  $80^\circ\text{C}$  for 3 h.

### 3.4. Recycling of Used $\text{CoFe}_2\text{O}_4\text{-Si-ASA}$ Nanocatalyst

Subsequently, the magnetic  $\text{CoFe}_2\text{O}_4\text{-Si-ASA}$  nanocatalyst used during the hydrolysis reaction was easily recovered by providing a magnetic field, which was further reused for the next cycles of the hydrolysis experiment. For recycling experiments, similar hydrolysis conditions were used as for the optimization studies (350 mg catalyst per g of substrate), hydrolyzed for 3 h at  $80^\circ\text{C}$ .

Reusability of the nanocatalyst was tested for three cycles of the hydrolysis experiment, as demonstrated in Figure 6. A minor decline in the hydrolytic performance was

observed during the recycling of the nanocatalyst for the second and third cycle. A trivial decrease in the production of daidzein and genistein, i.e., from 59 and 62.2% to 43.2 and 35%, respectively, was noted after the second recycling experiment. For the third recycling of the nanocatalyst, a further ~35% decrease in conversion efficiency was observed. These results indicated that the bond between sulfonic acid groups and silica-coated  $\text{CoFe}_2\text{O}_4$  catalyst remained strong even after reusing the nanocatalyst for hydrolysis reaction. However, the gradual decline in glycoside conversion was detected during subsequent cycles, which can be implicated to the loss of reacted/unreacted sulfonic acid groups on the silica surface [24,25]. The acidity of the reused nanocatalyst after the third cycle was calculated to be  $0.73 \text{ mM H}^+/\text{g}$ , which was less than that of the unused catalyst ( $0.92 \text{ mM H}^+/\text{g}$ ). Hence, the possible improvement in the process of functionalizing acid groups on MNPs to achieve stronger bonding can improve the catalytic efficiency of the nanocatalyst. However, the selectivity in terms of the generation of daidzein and genistein components was still maintained even after the last third recycle because of the occurrence of robust sulfonic acid functional groups, which are supposed to be catalytic sites for hydrolysis reaction. In view of these observations, it is clear that acid-functionalized nanocatalyst can prove to be one of the promising options for the generation of aglycone compounds by breaking down  $\beta$ -glycosidic linkages present in the glycosides.

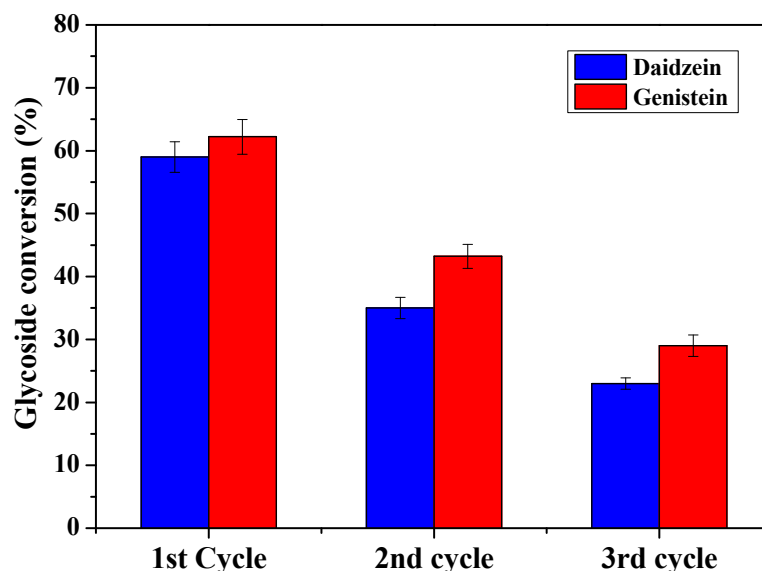


**Figure 6.** Recycling of used acid-functionalized cobalt ferrite alkyl sulfonic acid ( $\text{CoFe}_2\text{O}_4\text{-Si-ASA}$ ) nanocatalyst for a hydrolysis experiment. Hydrolysis reaction was performed at  $80^\circ\text{C}$  for 3 h.

#### 4. Conclusions

The synthesis of an acid-functionalized  $\text{CoFe}_2\text{O}_4\text{-Si-ASA}$  nanocatalyst possessing strong sulfonic acid groups was confirmed by characterization studies and the acid titration method. Hydrolysis of glycosides into aglycones was achieved with conversion efficiencies of 59.0–62.2% and 69.2–73.2% using  $\text{CoFe}_2\text{O}_4\text{-Si-ASA}$  nanocatalyst at  $80^\circ\text{C}$  for 3 h and  $120^\circ\text{C}$  with 15 psi pressure for 1 h, respectively. Most importantly, hydrolysis experiments were performed at a lower temperature ( $80^\circ\text{C}$ ) for only 3 h, which is promising for hydrolysis of glycosidic linkages in various substrates. In addition,  $\text{CoFe}_2\text{O}_4\text{-Si-ASA}$  nanocatalyst can be easily recovered and recycled because of its magnetic properties. In view of the expedient hydrolytic efficiency of these  $\text{CoFe}_2\text{O}_4\text{-Si-ASA}$  MNPs, it is assumed that such a nanocatalyst can be a better alternate candidate for conventional enzymes used for the breakdown of glycosidic linkages. Hitherto, no studies have been reported on the exploitation of such an acid-functionalized nanocatalyst,  $\text{CoFe}_2\text{O}_4\text{-Si-ASA}$ , for the generation of aglycones by converting glycoside moieties. Although few studies reported the use of solid acid catalysts for cellobiose conversion, reactions were performed

under extreme conditions (e.g., high temperature, high pressure, etc.) and for a longer period. On the contrary, the process standardized in the current study was conducted at considerably lower temperature and shorter reaction time, which makes the strategy more expedient. Moreover, the easy recovery of the magnetic nanocatalyst because of its magnetic property makes it possible to reuse the  $\text{CoFe}_2\text{O}_4\text{-Si-ASA}$  nanocatalyst for succeeding cycles of hydrolysis. All these parameters and accomplished outcomes from this study would certainly aid in making the process commercially viable by reducing the extensive cost involved in the process. Ultimately, this process can substantiate to be an effective unconventional approach for the synthesis of therapeutically relevant aglycone compounds on a commercial scale.

**Supplementary Materials:** The following supporting information can be downloaded at <https://www.mdpi.com/article/10.3390/catal12101107/s1>: Figure S1: SEM (A and B) and TEM (C and D) analysis of cobalt ferrite ( $\text{CoFe}_2\text{O}_4$ ) and silica coated of cobalt ferrite ( $\text{CoFe}_2\text{O}_4\text{-Si}$ ) nanocatalyst, respectively; Figure S2: EDX analysis of the synthesized nanoparticles: (A) cobalt ferrite ( $\text{CoFe}_2\text{O}_4$ ), (B) silica coated of cobalt ferrite ( $\text{CoFe}_2\text{O}_4\text{-Si}$ ), and (C) acid-functionalized cobalt ferrite alkyl sulfonic acid ( $\text{CoFe}_2\text{O}_4\text{-Si-ASA}$ ); Figure S3: Cobalt ferrite ( $\text{CoFe}_2\text{O}_4$ ) nanoparticles showing magnetic property; Figure S4:  $\text{CoFe}_2\text{O}_4$  MNPs showing magnetic property.

**Author Contributions:** Conceptualization, M.S.; methodology, M.S. and M.K.; formal analysis, M.S.; investigation, M.S.; data curation, M.S.; writing—original draft preparation, M.S.; writing—review and editing, B.-S.K.; supervision, B.-S.K. All authors have read and agreed to the published version of the manuscript.

**Funding:** This research was funded by the National Research Foundation of Korea (NRF- 2021R1I1A1A01043785).

**Institutional Review Board Statement:** Not applicable.

**Informed Consent Statement:** Not applicable.

**Data Availability Statement:** Data is available upon request.

**Conflicts of Interest:** The authors declare that they have no competing interest to the reported studies in this paper.

## References

1. Albertazzi, P.; Purdie, D.W. The nature and utility of the phytoestrogens: A review of the evidence. *Maturitas* **2002**, *42*, 173–185. [[CrossRef](#)]
2. Nemitz, M.C.; Picada, J.N.; da Silva, J.; Garcia, A.L.H.; Papke, D.K.; Grivicich, I.; Teixeira, H.F. Determination of the main impurities formed after acid hydrolysis of soybean extracts and the in vitro mutagenicity and genotoxicity studies of 5-ethoxymethyl-2-furfural. *J. Pharm. Biomed. Anal.* **2016**, *129*, 427–432. [[CrossRef](#)]
3. Křížová, L.; Dadáková, K.; Kašparovská, J.; Kašparovský, T. Isoflavones. *Molecules* **2019**, *24*, 1076. [[CrossRef](#)]
4. Barnes, S. The biochemistry, chemistry and physiology of the isoflavones in soybeans and their food products. *Lymphat. Res. Biol.* **2010**, *8*, 89–98. [[CrossRef](#)]
5. He, F.J.; Chen, J.Q. Consumption of soybean, soy foods, soy isoflavones and breast cancer incidence: Differences between Chinese women and women in Western countries and possible mechanisms. *Food Sci. Hum. Wellness* **2013**, *2*, 146–161. [[CrossRef](#)]
6. Halabalaki, M.; Alexi, X.; Aligiannis, N.; Lambrinidis, G.; Pratsinis, H.; Florentin, I.; Mitakou, S.; Mikros, E.; Skaltsounis, A.-L.; Alexis, M.N.; et al. Estrogenic activity of isoflavonoids from *Onobrychis ebenoides*. *Planta Med.* **2006**, *72*, 488–493. [[CrossRef](#)]
7. Paterni, I.; Granchi, C.; Katzenellenbogen, J.A.; Minutolo, F. Estrogen receptors alpha ( $\text{ER}\alpha$ ) and beta ( $\text{ER}\beta$ ): Subtype-selective ligands and clinical potential. *Steroids* **2014**, *90*, 13–29. [[CrossRef](#)]
8. Sathyapalan, T.; Aye, M.; Rigby, A.S.; Thatcher, N.J.; Dargham, S.R.; Kilpatrick, E.S.; Atkin, S.L. Soy isoflavones improve cardiovascular disease risk markers in women during the early menopause. *Nutr. Metab. Cardiovasc. Dis.* **2018**, *28*, 691–697. [[CrossRef](#)]
9. Hillman, G.G.; Singh-Gupta, V.; Al-Bashir, A.K.; Yunker, C.K.; Joiner, M.C.; Sarkar, F.H.; Abrams, J.; Mark Haacke, E. Monitoring sunitinib-induced vascular effects to optimize radiotherapy combined with soy isoflavones in murine xenograft tumor. *Transl. Oncol.* **2011**, *4*, 110–121. [[CrossRef](#)]
10. Ullah, A.; Munir, S.; Badshah, S.L.; Khan, N.; Ghani, L.; Poulson, B.G.; Emwas, A.H.; Jaremko, M. Important flavonoids and their role as a therapeutic agent. *Molecules* **2020**, *25*, 5243. [[CrossRef](#)]

11. Chen, P.X.; Tang, Y.; Zhang, B.; Liu, R.; Marcone, M.F.; Li, X.; Tsao, R. 5-Hydroxymethyl-2-furfural and derivatives formed during acid hydrolysis of conjugated and bound phenolics in plant foods and the effects on phenolic content and antioxidant capacity. *J. Agric. Food Chem.* **2014**, *62*, 4754–4761. [[CrossRef](#)]
12. Nemitz, M.C.; Moraes, R.C.; Koester, L.S.; Bassani, V.L.; von Poser, G.L.; Teixeira, H.F. Bioactive soy isoflavones: Extraction and purification procedures, potential dermal use and nanotechnology-based delivery systems. *Phytochem. Rev.* **2015**, *14*, 849–869. [[CrossRef](#)]
13. Chang, K.H.; Jo, M.N.; Kim, K.T.; Paik, H.D. Evaluation of glucosidases of *Aspergillus niger* strain comparing with other glucosidases in transformation of ginsenoside Rb1 to ginsenosides Rg3. *J. Ginseng Res.* **2014**, *38*, 47–51. [[CrossRef](#)]
14. Feng, C.; Jin, S.; Xia, X.X.; Guan, Y.; Luo, M.; Zu, Y.G.; Fu, Y.J. Effective bioconversion of sophoricoside to genistein from *Fructus sophorae* using immobilized *Aspergillus niger* and yeast. *World J. Microbiol. Biotechnol.* **2015**, *31*, 187–197. [[CrossRef](#)]
15. Gaya, P.; Peiroten, A.; Medina, M.; Landete, J.M. Isoflavone metabolism by a collection of lactic acid bacteria and bifidobacteria with biotechnological interest. *Int. J. Food Sci. Nutr.* **2016**, *67*, 117–124. [[CrossRef](#)]
16. Singhvi, M.S.; Zinjarde, S.S. Production of pharmaceutically important genistein and daidzein from soybean flour extract by using  $\beta$ -glucosidase derived from *Penicillium janthinellum* NCIM 1171. *Process Biochem.* **2020**, *97*, 183–190. [[CrossRef](#)]
17. Liu, F.; Huang, K.; Zheng, A.; Xiao, F.S.; Dai, S. Hydrophobic solid acids and their catalytic applications in green and sustainable chemistry. *ACS Catal.* **2018**, *8*, 372–391. [[CrossRef](#)]
18. Zhou, Y.; Noshadi, I.; Ding, H.; Liu, J.; Parnas, R.S.; Clearfield, A.; Xiao, M.; Meng, Y.; Sun, L. Solid acid catalyst based on single-layer  $\alpha$ -zirconium phosphate nanosheets for biodiesel production via esterification. *Catalysts* **2018**, *8*, 17. [[CrossRef](#)]
19. Peña, L.; Xu, F.; Hohn, K.L.; Li, J.; Wang, D. Propyl-sulfonic acid functionalized nanoparticles as catalyst for pretreatment of corn stover. *J. Biomater. Nanobiotechnol.* **2014**, *5*, 8–16. [[CrossRef](#)]
20. Qi, W.; He, C.; Wang, Q.; Liu, S.; Yu, Q.; Wang, W.; Leksawasdi, N.; Wang, C.; Yuan, Z. Carbon-based solid acid pretreatment in corncob saccharification: Specific xylose production and efficient enzymatic hydrolysis. *ACS Sustain. Chem. Eng.* **2018**, *6*, 3640–3648. [[CrossRef](#)]
21. Peña, L.; Ikenberry, M.; Ware, B.; Hohn, K.L.; Boyle, D.; Sun, X.S.; Wang, D. Cellobiose hydrolysis using acid-functionalized nanoparticles. *Biotechnol. Bioprocess Eng.* **2011**, *16*, 1214–1222. [[CrossRef](#)]
22. Carlier, S.; Hermans, S. Highly efficient and recyclable catalysts for cellobiose hydrolysis: Systematic comparison of carbon nanomaterials functionalized with benzyl sulfonic acids. *Front. Chem.* **2020**, *8*, 347. [[CrossRef](#)]
23. Singhvi, M.S.; Deshmukh, A.R.; Kim, B.S. Cellulase mimicking nanomaterial-assisted cellulose hydrolysis for enhanced bioethanol fermentation: An emerging sustainable approach. *Green Chem.* **2021**, *23*, 5064–5081. [[CrossRef](#)]
24. Wang, D.; Ikenberry, M.; Pe, L.; Hohn, K.L. Acid-functionalized nanoparticles for pretreatment of wheat straw. *J. Biomater. Nanobiotechnol.* **2012**, *3*, 342–352. [[CrossRef](#)]
25. Ingle, A.P.; Philippini, R.R.; de Souza Melo, Y.C.; da Silva, S.S. Acid-functionalized magnetic nanocatalysts mediated pretreatment of sugarcane straw: An eco-friendly and cost-effective approach. *Cellulose* **2020**, *27*, 7067–7078. [[CrossRef](#)]
26. Rajkumari, K.; Kalita, J.; Das, D.; Rokhum, L. Magnetic Fe<sub>3</sub>O<sub>4</sub>@ silica sulfuric acid nanoparticles promoted regioselective protection/deprotection of alcohols with dihydropyran under solvent-free conditions. *RSC Adv.* **2017**, *7*, 56559–56565. [[CrossRef](#)]
27. Melero, J.A.; Stucky, G.D.; van Grieken, R.; Morales, G. Direct syntheses of ordered SBA-15 mesoporous materials containing arenesulfonic acid groups. *J. Mater. Chem.* **2002**, *12*, 1664–1670. [[CrossRef](#)]
28. Walker, J.M. The bicinchoninic acid (BCA) assay for protein quantitation. *Methods Mol. Biol.* **1994**, *32*, 5–8. [[CrossRef](#)]
29. Maharjan, A.; Singhvi, M.; Kim, B.S. Biosynthesis of a therapeutically important nicotinamide mononucleotide through a phosphoribosyl pyrophosphate synthetase 1 and 2 engineered strain of *Escherichia Coli*. *ACS Synth. Biol.* **2021**, *10*, 3055–3065. [[CrossRef](#)]
30. Tanuraghaj, H.M.; Farahi, M. Preparation, characterization and catalytic application of nano-Fe<sub>3</sub>O<sub>4</sub>@ SiO<sub>2</sub>@(CH<sub>2</sub>)<sub>3</sub>OCO<sub>2</sub>Na as a novel basic magnetic nanocatalyst for the synthesis of new pyranocoumarin derivatives. *RSC Adv.* **2018**, *8*, 27818–27824. [[CrossRef](#)]
31. Safari, J.; Zarnegar, Z. A magnetic nanoparticle-supported sulfuric acid as a highly efficient and reusable catalyst for rapid synthesis of amidoalkyl naphthols. *J. Mol. Catal. A Chem.* **2013**, *379*, 269–276. [[CrossRef](#)]
32. Colilla, M.; Izquierdo-Barba, I.; Sánchez-Salcedo, S.; Fierro, J.L.; Hueso, J.L.; Vallet-Regí, M. Synthesis and characterization of zwitterionic SBA-15 nanostructured materials. *Chem. Mater.* **2010**, *22*, 6459–6466. [[CrossRef](#)]
33. Alvaro, M.; Corma, A.; Das, D.; Fornés, V.; García, H. “Nafion”-functionalized mesoporous MCM-41 silica shows high activity and selectivity for carboxylic acid esterification and Friedel–Crafts acylation reactions. *J. Catal.* **2005**, *231*, 48–55. [[CrossRef](#)]
34. Ramanathan, G.; Banupriya, S.; Abirami, D. Production and optimization of cellulase from *Fusarium oxysporum* by submerged fermentation. *J. Sci. Ind. Res.* **2010**, *69*, 454–459.
35. De Almeida, M.N.; Falkoski, D.L.; Guimarães, V.M.; de Rezende, S.T. Study of gamba grass as carbon source for cellulase production by *Fusarium verticillioides* and its application on sugarcane bagasse saccharification. *Ind. Crops Prod.* **2019**, *133*, 33–43. [[CrossRef](#)]
36. Izumi, T.; Piskula, M.K.; Osawa, S.; Obata, A.; Tobe, K.; Saito, M.; Kataoka, S.; Kubota, Y.; Kikuchi, M. Soy isoflavone aglycones are absorbed faster and in higher amounts than their glucosides in humans. *J. Nutr.* **2000**, *130*, 1695–1699. [[CrossRef](#)]
37. Hu, S.; Wang, D.; Hong, J. A simple method for beta-glucosidase immobilization and its application in soybean isoflavone glycosides hydrolysis. *Biotechnol. Bioprocess Eng.* **2018**, *23*, 39–48. [[CrossRef](#)]

38. Mei, J.; Chen, X.; Liu, J.; Yi, Y.; Zhang, Y.; Ying, G. A biotransformation process for production of genistein from sophoricoside by a strain of *Rhizopus oryza*. *Sci. Rep.* **2019**, *9*, 6564. [[CrossRef](#)]
39. Doan, D.T.; Luu, D.P.; Nguyen, T.D.; Hoang Thi, B.; Pham Thi, H.M.; Do, H.N.; Luu, V.H.; Pham, T.D.; Than, V.T.; Thi, H.H.P.; et al. Isolation of *Penicillium citrinum* from roots of *Clerodendron cyrtophyllum* and application in biosynthesis of aglycone isoflavones from soybean waste fermentation. *Foods* **2019**, *8*, 554. [[CrossRef](#)]
40. Wang, H.; Covarrubias, J.; Prock, H.; Wu, X.; Wang, D.; Bossmann, S.H. Acid-functionalized magnetic nanoparticle as heterogeneous catalysts for biodiesel synthesis. *J. Phys. Chem. C* **2015**, *119*, 26020–26028. [[CrossRef](#)]